NJBAS

Available online at http://www.ajol.info/index.php/njbas/index
Nigerian Journal of Basic and Applied Science (December, 2012), 20(4): 327-340

ISSN 0794-5698

Full Length Research Article

Boundary Layer Fluid Flow in a Channel with Heat Source, Soret Effects and Slip Condition

I. J. Uwanta, *B.Y. Isah
***Department of Mathematics, Usmanu Danfodiyo University. Sokoto, Nigeria**
[Corresponding Author: E-Mail: isahbyabo@yahoo.com; ☎: +234(0)8068062727]

ABSTRACT: The boundary layer fluid flow in a channel with heat source, soret effects and slip condition was studied. The governing equations were solved using perturbation technique. The effects of different parameters such Prandtl number Pr, Hartmann number M, Schmidt number Sc, suction parameter λ, soret number Sr and the heat source s on velocity, temperature and concentration were studied. Numerical computations involved in the solution have been shown on graphs and tables. It was observed that the temperature increased with an increase in perturbation parameter, heat source, and suction, but temperature decrease with increase in Prandtl numbers. The concentration profile increased with an increasing suction, soret, and perturbation parameter and decreases with an increasing Schmidt and heat source parameters, while the velocity increased with increase in Hartmann number, perturbation parameter, suction, Grashof and modified Grashof numbers, and slip variable and decreased as a result of an increasing Schmidt, Prandtl and soret numbers. The skin friction coefficient, Nusselt number and Sherwood number were also depicted on tables. The skin friction coefficient increased with the increase in material parameters $\lambda, Pr, Sc, Sr, Gc, \text{and}\, mt$ and decreased with increase of material parameters $s, Gr, M, \text{and}\, \gamma$. Increasing effects of Pr, decreased the Nusselt number while increasing $\lambda, s\, \text{and}\, mt$ increased the Nusselt number with appreciative results. Sherwood number increased with the increased of material parameter Pr and inversely decreases with increase in $s\; s, \lambda, Sc, Sr\, \text{and}\, mt$.

Keywords: Heat source, soret, boundary layer, channel, perturbation, slip condition

INTRODUCTION

Fundamental studies of boundary layer fluid flow problem attract the interest of engineering sciences, applied mathematics researchers and geophysical application such as geothermal reservoirs, thermal insulation, enhanced oil recovery, packed-bed catalytic reactors, cooling of nuclear reactors, metallurgical and polymer extrusion processes. In a pioneering work, Sakiadis (1961) investigated the boundary layer flow induced by a moving plate in a quiescent ambient fluid. Thereafter, various aspects of the problem have been investigated by many authors. Makinde and Aziz (2011) reported that, the fluid flow over a stretching surface is important in applications such as extrusion, wire drawing, metal spinning and hot rolling. It is crucial to understand the heat and flow characteristics of the process so that the finished product meets the desired quality specifications. A wide variety of problems dealing with heat and fluid flow over a stretching sheet have been studied with both Newtonian and non-Newtonian fluids and with the inclusion of imposed electric and magnetic fields, different thermal boundary conditions, and power law variation of the stretching velocity. Ching-Yang Cheng (2010) presented the analysis of the Soret and Dufour effects on the boundary layer flow due to free convection heat and mass transfer over a cylinder in a porous medium with constant wall temperature and concentration. Due to the great importance of soret (thermal diffusion) and Dufour (Diffusion Thermo), Anjali *et al.* (2002) and Postelnicu (2004) reported results effects of soret and Dufour on fluid flow with very light molecular weight as well as medium molecular weight. Er-Raki *et al.* (2010) studied the soret effect on double-diffusion boundary layer flows in a vertical porous layer. Alam *et al.* (2005) studied the Dufour and Soret effects on steady MHD free convective heat and mass transfer flow pass a semi-infinite vertical porous plate embedded in a porous medium. Alam *et al.* (2006) studied the Dufour and Soret effects on unsteady free convective and mass transfer flow past an impulsively started infinite vertical porous flat plate in a porous medium under the influence of transversely applied magnetic field. Stanford *et al.* (2010) investigated the influence of a magnetic field on heat and mass transfer by mixed convection from vertical surface in the presence of Hall, radiation, soret (thermal- diffusion) and (diffusion-thermo) effect. Effect of heat and mass transfer on nonlinear MHD boundary layer flow has been discussed (Brady and Acrivos, 1981; Cheng and Lin, 2002; Kuo, 2005). Muhaimin *et al.* (2009) studied the effect of chemical reaction, heat and mass transfer on a nonlinear MHD boundary layer past a porous shrinking sheet in the Presence of suction. Vajravelu and Hadjinicolaou (1999) studied the heat transfer characteristics in the laminar boundary layer of a viscous fluid over a stretching sheet with viscous dissipation or frictional heating and internal heat generation. Cortell (2008) studied the effects of viscous dissipation and radiation on the thermal boundary layer over a nonlinearly stretching sheet. Postelnicu (2004) studied the influence of a magnetic field on heat and mass transfer by natural convection from vertical surface embedded in an electrically conducting fluid saturated porous media considering Soret and Dufour effects with constant surface temperature and concentration. Alam *et al*. (2006) studied the Dufour and Soret effects on steady MHD combined free-forced convective and mass transfer flow past a semi-infinite vertical plate. Makinde and Olanrewaju (2011) investigated the unsteady mixed convection flow past a vertical porous flat plate moving through a binary mixture in the presence of Radiative heat transfer and nth-order Arrhenius type of irreversible chemical reaction by taking into account the diffusion-thermal (Dufour) and thermo-diffusion (Soret) effects.

Problem Formulation

The authors consider the region of unsteady MHD flow of boundary layer fluid with heat source, soret effect and slip variable on incompressible, electrically conducting fluid over a finite region perpendicular to a finite vertical plate h moving with constant velocity, U, in the presence of a transverse magnetic field. The surface temperatures of the plate oscillates with small amplitude about a non-uniform mean temperature. The x-axis is taken along the plate ad the y-axis is normal to the plate. The governing equations are the continuity equation momentum, energy and concentration.

$$\frac{\partial v'}{\partial y'} = 0 \tag{1a}$$

$$\frac{\partial u'}{\partial t'} - v'\frac{\partial u'}{\partial y'} = -\frac{\partial p'}{\partial x'} + v\frac{\partial^2 u'}{\partial y'^2} - \frac{\sigma_e B_0^2 u'}{\rho} + g\beta(T' - T_0') + g\beta^*\left(C' - C_0'\right) \tag{1b}$$

$$\frac{\partial T'}{\partial t'} - v'\frac{\partial u'}{\partial y'} = \frac{k}{\rho C_p}\frac{\partial^2 T'}{\partial y'^2} + \frac{\theta_0(T' - T_0')}{\rho C_p} \tag{2}$$

$$\frac{\partial C'}{\partial t'} - v'\frac{\partial C'}{\partial y'} = D^*\frac{\partial^2 C'}{\partial y'^2} + \frac{DT}{\rho C_p}\frac{\partial^2 T'}{\partial y'^2} \tag{3}$$

and the boundary conditions

$$\left.\begin{array}{ll} u' - \lambda\dfrac{\partial u'}{\partial y'} = o, \quad \theta_0 = 0, \quad C = 0 & at\, y = 0 \\ u' = 0, \quad T' = T_W' + (T_W' - T_0')\varepsilon e^{i\omega t}, C' = \left(C_W' - C_0'\right)\varepsilon e^{i\omega t} & at\, y = h \end{array}\right\} \tag{4}$$

where x' and y' are the dimensional distances along and perpendicular to the plate respectively, u', v' are the components of dimensional velocities along x' and y' respectively, ρ is the fluid density, *V* is the fluid kinematic viscosity, *g* is the acceleration due to gravity, β and β_c are the coefficients of volume expansions for temperature and concentration respectively, k is thermal conductivity, σ is the electrical conductivity of the fluid, B_0 is the magnetic induction, γ is slip variable , *T* is the temperature, C' is the component of dimensional concentration, *D* is the coefficient of mass diffusivity, ε is the material parameter , v_0 is a scale of suction velocity which has non-zero positive constant.

The flow is normalized with the following dimensionless quantities:

$$\left\{ x = \frac{x'}{a}, y = \frac{y'}{a}, u = \frac{u'}{u}, \theta = \frac{T' - T'_0}{T'_w - T'_0}, C = \frac{C' - C'_0}{C'_w - C'_0}, M^2 = \frac{a^2 \sigma_e B_0^2}{\sigma v}, t = \frac{t'u}{a}, \right.$$

$$\left. p = \frac{ap'}{\rho v u}, Gr = \frac{g\beta(T'_w - T_0)a^2}{vu}, Pr = \frac{v\rho C_p}{k}, Sc = \frac{v}{D^*}, Sr = \frac{D_T}{T_w v}, \lambda = \frac{v_0 a}{v} \right\} \tag{5}$$

the governing equations(1) to (4) were reduced into dimensionless form by using (5) as:

$$\frac{\partial u}{\partial t} - \lambda \frac{\partial u}{\partial y} = -\frac{\partial p}{\partial x} + \frac{\partial^2 u}{\partial y^2} - M^2 u + Gr\theta + GcC \tag{6}$$

$$\frac{\partial \theta}{\partial t} - \lambda \frac{\partial \theta}{\partial y} = \frac{1}{Pr}\frac{\partial^2 \theta}{\partial y^2} + \theta s \tag{7}$$

$$\frac{\partial C}{\partial t} - \lambda \frac{\partial C}{\partial y} = \frac{1}{Sc}\frac{\partial^2 C}{\partial y^2} + Sr\frac{\partial^2 \theta}{\partial y^2} \tag{8}$$

With the corresponding boundary conditions;

$$\left. \begin{array}{l} u - \gamma u' = 0, \quad \theta = 0, \quad\quad C = 0 \quad at \;\; y = 0 \\ u = 0, \;\; \theta = 1 + \varepsilon e^{mt}, \;\; C = 1 + \varepsilon e^{mt} \quad at \;\; y = h \end{array} \right\} \tag{9}$$

Assuming the pressure term as

$$\frac{\partial p}{\partial x} = A + B\varepsilon e^{mt} \tag{10}$$

where A and B are constants, Pr is Prandtl number, M is Hartmann number, Sc is Schmidt number, λ is suction parameter, Sr is soret number and s is the heat source.

METHOD OF SOLUTION

In order to reduce the above system of partial differential equations to a system of ordinary differential equations in dimensionless form, Let the assumed solution of the velocity, temperature and mass be taken as:

$$\left. \begin{array}{l} u(y,t) = u_0(y) + \varepsilon e^{mt} u_1(y) + O(\varepsilon^2) \\ \theta(y,t) = \theta_0(y) + \varepsilon e^{mt} \theta_1(y) + O(\varepsilon^2) \\ C(y,t) = C_0(y) + \varepsilon e^{mt} C_1(y) + O(\varepsilon^2) \end{array} \right\} \tag{11}$$

Substituting (10) and (11) and collecting harmonic terms then;

$$\frac{\partial u_0}{\partial y} + \lambda \frac{\partial u_0}{\partial y} - M^2 u_0 = A - Gr\theta_0 - GcC_0 \tag{12}$$

$$\frac{\partial^2 \theta_0}{\partial y^2} + \lambda Pr \frac{\partial \theta_0}{\partial y} + sPr = 0 \tag{13}$$

$$\frac{\partial^2 C_0}{\partial y^2} + \lambda Sc \frac{\partial C_0}{\partial y} + sPr = -SrSc\frac{\partial^2 \theta_0}{\partial y^2} \tag{14}$$

$$\frac{d^2 u_1}{dy^2} + \lambda \frac{du_1}{dy} - \left(M^2 + m\right) u_1 = B - Gr\theta - GcC_1 \tag{15}$$

$$\frac{d^2\theta_1}{dy^2} + \lambda \frac{d\theta_1}{dy} + \Pr\theta_1 + (s - m)u_1 = B - Gr\theta - GcC_1 \tag{16}$$

$$\frac{d^2C_1}{dy^2} + \frac{\lambda ScdC_1}{dy} - mScC_1 = -\frac{ScS_r d^2\theta_1}{dy^2} \tag{17}$$

The boundary conditions are

$$\left.\begin{array}{ll} u_0 - \gamma u_0' = 0, \theta_0 = 0, C_0 = 0 & \text{at } y = 0 \\ u_0 = 0, \theta_0 = 1, C_0 = 1 & \text{at } y = h \\ u_1 - \gamma u_1' = 0, \theta_1 = 0, C_1 = 0 & \text{at } y = 0 \\ u_1 = 0, \theta_1 = 1, C_1 = 1 & \text{at } y = h \end{array}\right\} \tag{18}$$

The analytic solution of the dimensionless differential equations (13) to (18) subject to (19) are:

3.1 The solution of steady state

$$u_0(y) = D_1 e^{k_1 y} + D_2 e^{-k_2 y} + q_1 + q_2 e^{-a_1 y} + q_3 e^{-a_2 y} + q_4 e^{-y} \tag{19}$$

$$\theta_0(y) = A_1 e^{a_1 y} + A_2 e^{-a_2 y} \tag{20}$$

$$C_0(y) = A_5 + A_6 e^{-y} + A_7 e^{a_1 y} + A_8 e^{-a_2 y} \tag{21}$$

where

$$D_1 = \frac{\gamma k_2 D_2 - D_2}{1 - \gamma k_1} + \frac{C_3}{1 - \gamma k_1}, \quad k_1 = \frac{\left[-\lambda + \sqrt{\lambda^2 + 4m^2}\right]}{2}, \quad k_2 = \frac{\left[\lambda + \sqrt{\lambda^2 + 4m^2}\right]}{2}$$

$$C_3 = \left(-q_1 - q_2 - q_3 - q_4 - \gamma a_1 q_2 + \gamma a_2 q_3 - \gamma q_4\right), \quad N_1 = -ScS_r a_1^2 A_1, N_2 = -ScS_r a_2^2 A_2$$

$$C_4 = \frac{\left(-q_1 - q_2 e^{a_1 h} - q_3 e^{-a_2 h} - q_4 e^{-h}\right)}{e^{k_1 h}}, \quad D_2 = \frac{C_3 e^{k_1 h} - C_4 (1 - \gamma k_1) e^{k_1 h}}{(1 - \gamma k_1) e^{-k_2 h} - (\gamma k_2 - 1) e^{k_1 h}},$$

$$a_1 = \frac{1}{2}\left(-\lambda \Pr + \left(\lambda^2 \Pr^2 - 4s\Pr\right)^{\frac{1}{2}}\right), a_2 = \frac{1}{2}\left(\lambda \Pr + \left(\lambda^2 \Pr^2 - 4s\Pr\right)^{\frac{1}{2}}\right)$$

$$A_1 = -\frac{1}{e^{-a_2 h} - e^{a_1 h}}, A_2 = \frac{1}{e^{-a_2 h} - e^{a_1 h}}, \quad A_7 = \frac{N_1}{a_1^2 + \lambda Sca_1} \quad A_8 = \frac{N_2}{a_1^2 + \lambda Sca_2}$$

$$A_6 = \frac{1 - A_7\left(e^{a_1 h} - 1\right) - A_8\left(e^{-a_2 h} - 1\right)}{e^{-h} - 1}, \quad A_5 = -A_6 - A_7 - A_8$$

3.2 The solution of unsteady state

$$u_1 = L_1 e^{f_1 y} + L_2 e^{-f_2 y} + s_0 + s_1 e^{b_1 y} + s_2 e^{-b_2 y} + s_3 e^{d_1 y} + s_4 e^{-d_2 y} \tag{22}$$

$$\theta_1(y) = A_3 e^{b_1 y} + A_4 e^{-b_2 y} \tag{23}$$

$$C_1(y) = A_9 e^{d_1 y} + A_{10} e^{-d_2 y} + H_4 e^{b_1 y} + H_5 e^{-b_2 y} \tag{24}$$

where;

$$A_3 = -\frac{1}{e^{-b_2 h} - e^{b_1 h}}, A_4 = \frac{1}{e^{-b_2 h} - e^{b_1 h}} \quad N_3 = -ScS_r b_1^2 A_3 \text{ and } N_4 = -ScS_r b_2^2 A_4$$

$d_1 = \frac{1}{2}\left[-\lambda Sc + \left(-\lambda^2 Sc^2 + 4MSc \right)^{\frac{1}{2}} \right]$ and $d_2 = \frac{1}{2}\left[\lambda Sc + \left(-\lambda^2 Sc^2 + 4MSc \right)^{\frac{1}{2}} \right]$

$$H_4 = \frac{N_3}{b_1^2 + \lambda Sc b_1 - MSc},\ H_5 = \frac{N_4}{b_2^2 - \lambda Sc b_2 - MSc},\ A_{10} = \frac{1 - \left(e^{b_1 h} - e^{d_1 h} \right) H_4 - \left(e^{-b_2 h} - e^{d_1 h} \right) H_5}{e^{-d_2 h} - e^{d_1 h}}$$

$$A_9 = \frac{\left(e^{b_1 h} - e^{-d_2 h} \right) H_4 + \left(e^{-b_2 h} - e^{d_2 h} \right) H_5 - 1}{e^{-d_2 h} - e^{d_1 h}},\ f_1 = \frac{1}{2}\left[-1 + \left(1 + 4\left(M^2 + m \right) \right)^{\frac{1}{2}} \right],\ f_2 = \frac{1}{2}\left[1 + \left(1 + 4\left(M^2 + m \right) \right)^{\frac{1}{2}} \right]$$

$$s_0 = \frac{B}{M^2 - m}, s_1 = \frac{-GrA_3 - GcH_4}{b_1^2 + b_1 - M^2 - m}, s_2 = \frac{-GrA_4 - GcH_5}{b_2^2 - b_2 - M^2 - m},\quad s_3 = -\frac{GcA_9}{d_1^2 + d_1 - M^2 - m},$$

$$s_4 = -\frac{A_{10}Gc}{d_2^2 - d_2 - M^2 - m},\ L_1 = -\frac{\left(1 - \gamma f_2 \right) L_2}{1 - \gamma f_1} + \frac{C_1}{1 - \gamma f_1},\ L_2 = \frac{C_1 e^{f_1 h} - C_2 \left(1 - \gamma f_1 \right)}{\left(1 - \gamma f_2 \right) e^{f_1 h} - \left(1 - \gamma f_1 \right) e^{-f_2 h}}.$$

$$C_2 = -\left(s_0 + s_1 e^{b_1 h} + s_2 e^{-b_2 h} + s_3 e^{d_1 h} + s_4 e^{-d_2 h} \right)$$

In view of the equation (11), we obtain the stream wise, velocity, temperature and mass transfer fields as:

$$u(y) = D_1 e^{K_1 y} + D_2 e^{-K_2 y} + q_1 + q_2 e^{a_1 y} + q_3 e^{-a_2 y} + q_4 e^{-y} + \varepsilon \left[l_1 e^{f_1 y} + l_2 e^{-f_2 y} + s_0 + s_1 e^{b_1 y} + s_2 e^{-b_2 y} + s_3 e^{d_1 y} + s_4 e^{-d_2 y} \right] e^{mt} \tag{25}$$

$$\theta\left(y \right) = A_1 e^{a_1 y} + A_2 e^{-a_2 y} + \varepsilon \left[A_3 e^{b_1 y} + A_4 e^{-b_2 y} \right] e^{mt} \tag{26}$$

$$C\left(y \right) = A_5 + A_6 e^{-y} + A_7 e^{a_1 y} + A_8 e^{-a_2 y} + \varepsilon \left[A_9 e^{d_1 y} + A_{10} e^{-d_2 y} + H_4 e^{b_1 y} + H_5 e^{-b_2 y} \right] e^{mt} \tag{27}$$

3.3 Skin Friction, Rate of Heat and Mass Transfer

Skin-friction coefficient (τ) at the plate is:

$$\tau = -u'\left(y \right)\Big|_{y=0} \tag{28}$$

Heat transfer coefficient (Nu) at the plate is:

$$Nu = \theta'\left(y \right)\Big|_{y=0} \tag{29}$$

Mass transfer coefficient (Nu) at the plate is:

$$Sh = C'\left(y \right)\Big|_{y=0} \tag{30}$$

RESULTS AND DISCUSSION

In this frame, the variation of velocity field, temperature field, concentration field along y-axis, skin friction coefficient $\left(\tau\right)$, mass transfer coefficient in term of Nusselt number $\left(Nu\right)$ and Sherwood number $\left(Sh\right)$ were studied. To be realistic, the values of Prandtl number are chosen for water vapour $\left(Pr = 0.60\right)$, electrolytic solution $\left(Pr = 1.0\right)$, water $\left(Pr = 0.7\right)$, and water at $4^{0}C$ $\left(Pr = 11.4\right)$. The values of Schmidt number are chosen for hydrogen as $\left(Sc = 0.22\right)$, water-vapour $\left(Sc = 0.6\right)$, ammonia $\left(Sc = 0.78\right)$, methanol $\left(Sc = 1.0\right)$, and propyl benzene at $20^{0}C$ $\left(Sc = 2.62\right)$ as Shanker *et al.* (2010). The variation of temperature profile along y-axis are shown in Figures 1, 2, 3, 4 and 5 respectively for different values of perturbation parameter $(\varepsilon = 0.0, 0.2, 0.4, 0.6)$, Heat source ($s$ = 1.1,1.2,1.3) suction parameter $(\lambda = 0.3, 0.5, 0.7, 1.0)$, product of time and frequency oscillation $(mt = pi/6, pi/4, pi/3, pi/2)$, Prandtl number $(Pr = 0.6, 0.71, 0.85)$. It's shown that the temperature increases with increasing, perturbation, parameter ε, Heat source s, suction parameter λ, product of time and frequency oscillation mt but decrease with increase in Prandtl number Pr. The variation of the mass concentration along y-axis is presented in Figures 6 to 11 respectively for different varying values of Suction number $(\lambda = 0.3, 0.6, 0.7, 1.0)$, product of time and frequency oscillation $(mt = pi/6, pi/4, pi/3, pi/2)$, Soret number $(Sr = 1, 2, 5, 10)$, Schmidt number $(Sc = 0.6, 0.78, 1.0, 2.62)$, perturbation parameter $(\varepsilon = 0.02, 0.04, 0.08, 0.10)$. Heat source $(s = 0.4, 0.5, 0.6, 0.7)$. The results show that an increase in the suction number λ, product of time and frequency oscillation mt, soret number Sr, and perturbation parameter ε result to an increase in mass concentration and decreases with increasing Schmidt number Sc and Heat source s. The variation of velocity field along the y – axis shown in Figures 12 to 22 indicate the effects of Hartmann number $(M = 5, 6, 8, 10)$, perturbation parameter $(\varepsilon = 0.02, 0.2, 0.4, 0.6)$, product of time and frequency oscillation $(mt = pi/6, pi/4, pi/3, pi/2)$, Prandtl number $(Pr = 0.6, 0.71, 0.85)$, Schmidt number $(Sc = 0.22, 0.6, 0.78, 1.0)$, Soret number $(Sr = 0.0, 0.2, 0.5, 1.0)$, suction parameter $(\lambda = 0.3, 0.5, 0.7, 1.0)$, slip variable $(\gamma = 0.01, 0.05, 0.08, 0.10)$, mass Grashof number $(Gc = 5, 10, 15, 20)$, Grashof number $(Gr = 5, 10, 15, 20)$, and heat source (s = 1.1,1.2,1.3 1.4). It is observed that an increase in the Hartmann number M, perturbation parameter ε, product of time and frequency oscillation mt, suction parameter λ slip variable γ mass Grashof number Gc, Grashof number Gr and heat source s increases the velocity while an increase in Schmidt number Sc, Soret number Sr and Prandtl number Pr decreases the velocity.

Tables 1 – 3 represent the effect of Prandtl number Pr, Grashof number Gr, mass Grashof number Gc, suction parameter λ, heat source parameter s, product of time and frequency oscillation mt, soret number Sr and Hartmann magnetohydrodynamic number M and Schmidt number Sr on the skim friction coefficient τ, the heat transfer coefficient in term of Nusselt number Nu, and mass transfer coefficient in terms of Sherwood number Sh. In Table 1, it is observed that, an increase in $Pr, \lambda, Sc, Sr, Gc, and\ mt$ leads to increase in the value of skin-friction coefficient while an increase in $s, Gr, M, and\ \gamma$, leads to decrease in the value of skin friction coefficient. It is also seen from Table 2 that, the value of heat transfer coefficient increase with increasing $\lambda, and\ s$ while an increase in the Prandtl number leads to decrease in the value of heat transfer coefficient. The numerical values of mass transfer coefficient is also depict on Table 3 for different values of $Pr, \lambda, Sc, Sr,\ s\ and\ mt$ respectively. It is observed that, an increase in the Prandtl number leads to increase in the value of mass transfer coefficient while it decreases with increasing value of suction, heat source, Schmidt and soret numbers.

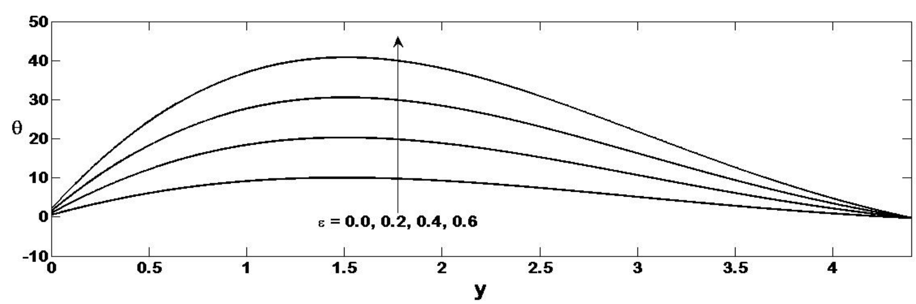

Figure 1: Effect of ε on temperature field θ when $mt = pi/2$ λ = 0.3, s = 0.1, Pr = 0.71

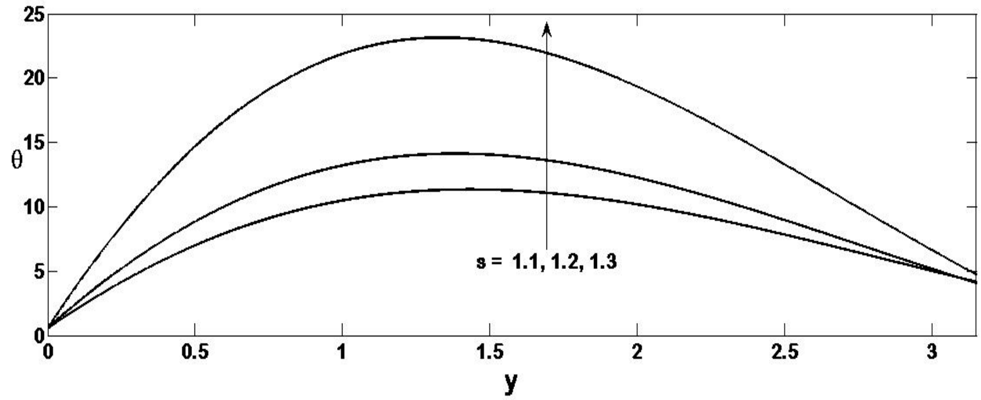

Figure 2: Effect of s on temperature field θ when $mt = pi/2$ λ = 0.3, ε = 0.02, Pr = 0.71

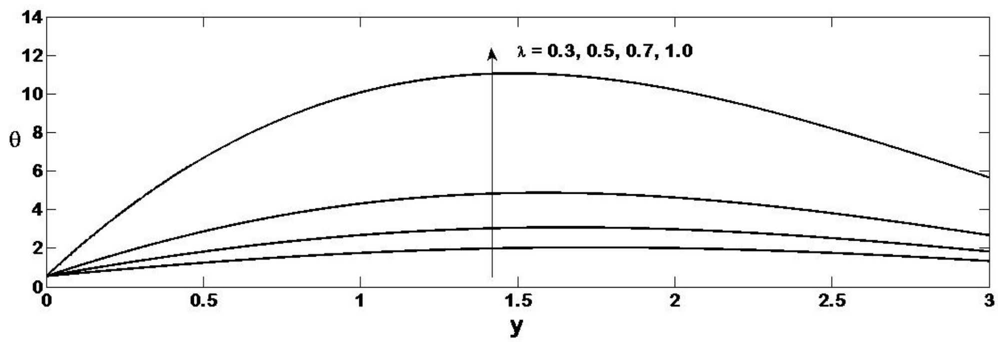

Figure 3: Effect of λ on temperature field θ when $mt = pi/2$, $s = 0.1$ ε = 0.02, Pr = 0.71

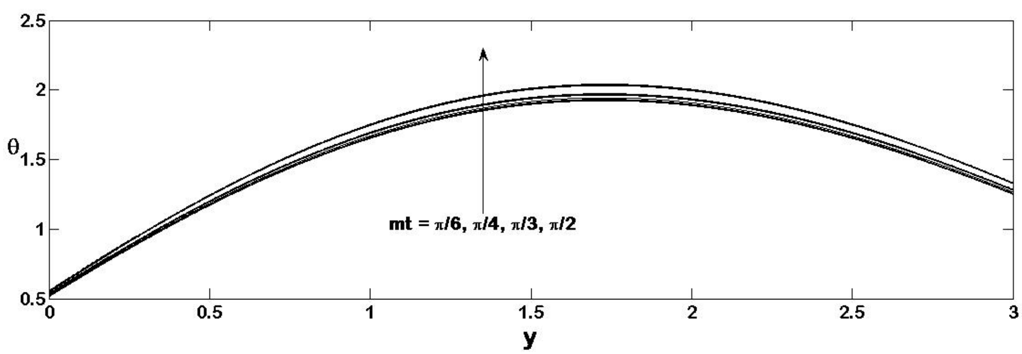

Figure 4: Effect of mt on temperature field θ when λ =0.3, s =0.1, ε = 0.02, Pr = 0.71.

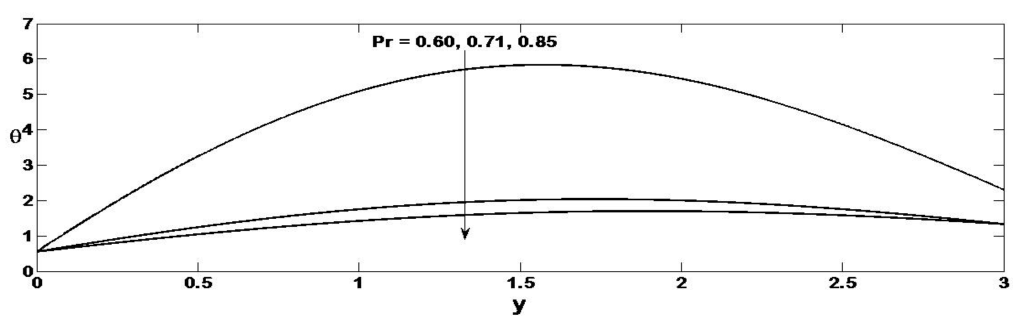

Figure 5: Effect of Pr on temperature field θ when λ =0.3, s =0.1, ε = 0.02, $mt = pi/2$

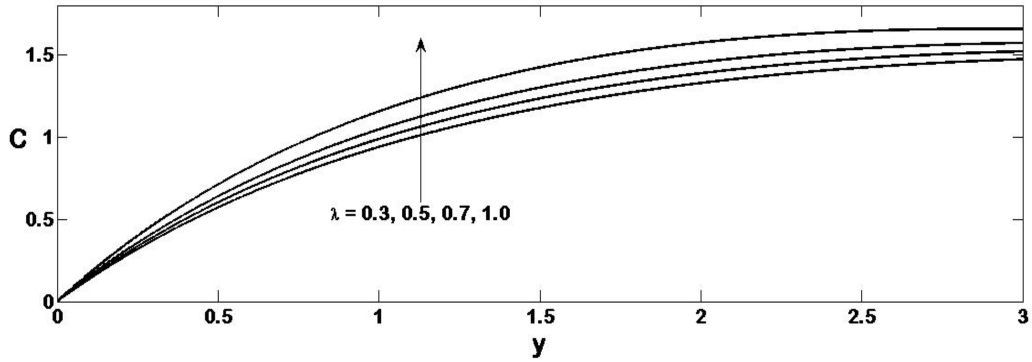

Figure 6: Effect of λ on concentration field C when ε = 0.02, = 0.3, Sc = 0.22, Sr = 0.2, $mt = pi/2$, $s = 0.1$

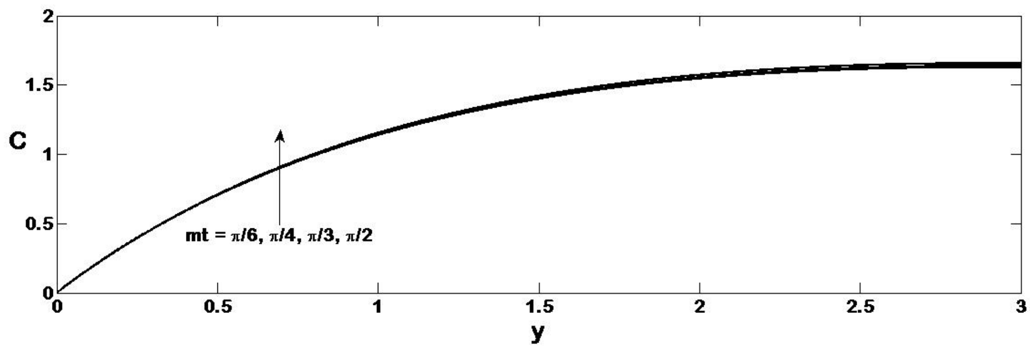

Figure 7: Effect of mt on concentration field C when ε = 0.02, = 0.3, Sc = 0.22, Sr = 0.2, λ = 0.3, s = 0.1

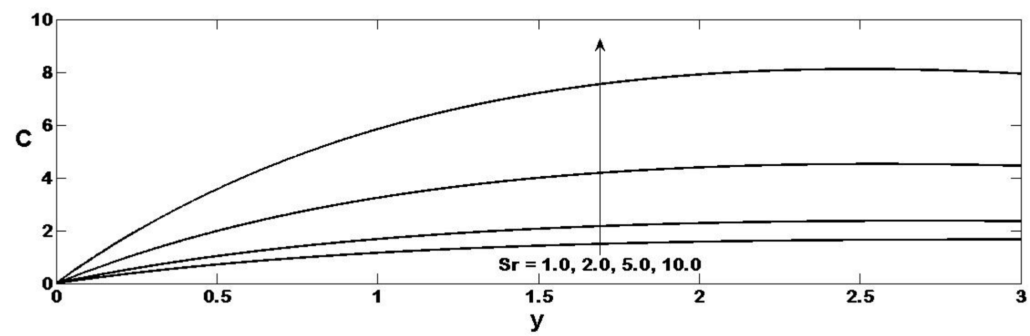

Figure 8: Effect of Sr on concentration field C when ε = 0.02, = 0.3, Sc = 0.22,$mt = pi/2$ λ = 0.3, s = 0.1

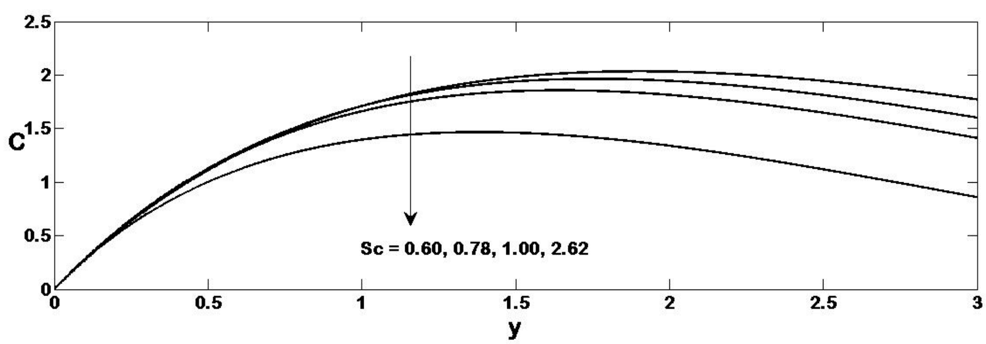

Figure 9: Effect of Sc on concentration field C when ε = 0.02, Sr = 0.2, $mt = pi/2$ λ = 0.3,s = 0.1

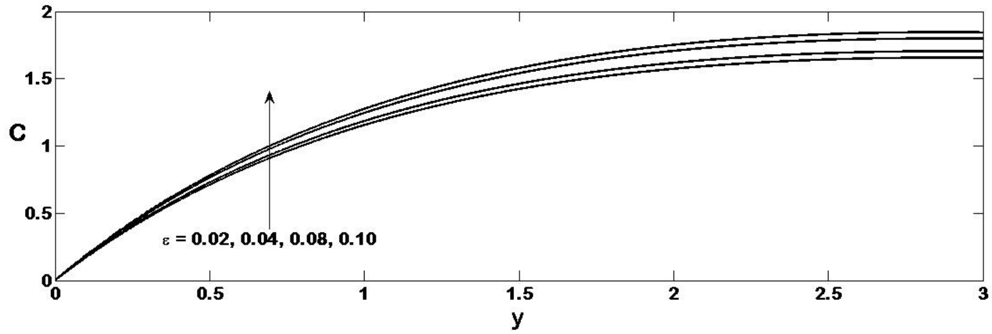

Figure 10: Effect of ε on concentration field C when $\lambda = 0.3$ Sr = 0.2, Sc =0.22, $s = 0.1$ $mt = pi/2$

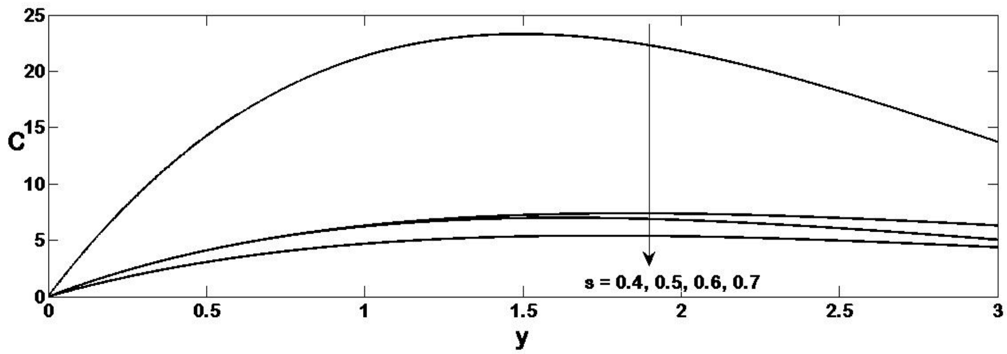

Figure 11: Effect of s on concentration field C when $\varepsilon = 0.02$, $\lambda = 0.3$, Sr = 0.2, Sc = 0.22, $mt = pi/2$

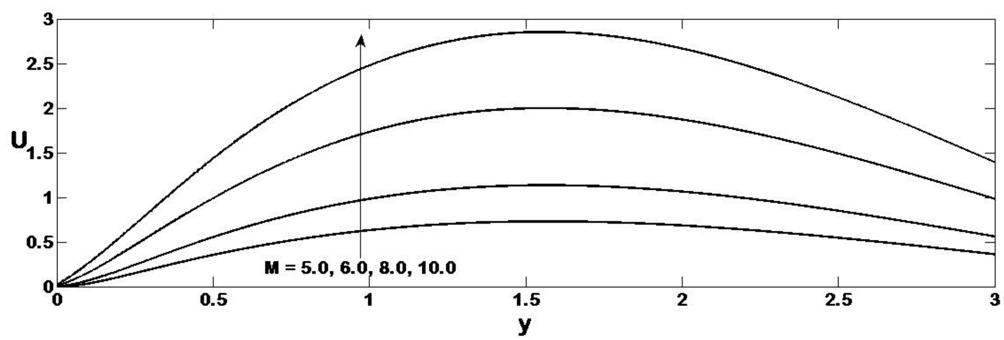

Figure 12: Effect of *M* on velocity field U for cooling of plate when Gc = 5, Gr = 5, Sr = 0.2, Sc = 0.22, Pr = 0.71, ε = 0.02, A = 0.1 = B, λ = 0.3, $s = 0.1$ $mt = pi/2$, $\gamma = 0.01$

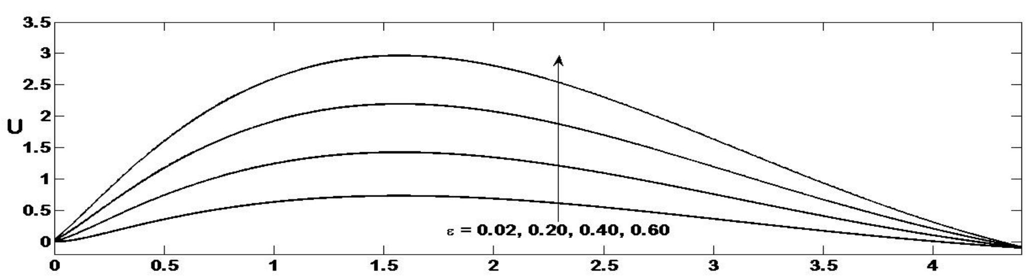

Figure 13: Effect of ε on velocity field U for cooling of plate when Gc = 5, Gr = 5, Sr = 0.2, Sc = 0.22, Pr = 0.71, M = 10, A = 0.1 = B, λ = 0.3,$\gamma = 0.01$ $s = 0.1$ $mt = pi/2$

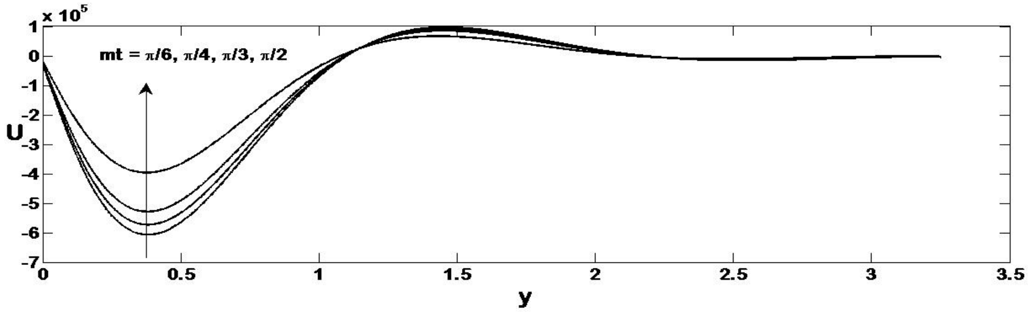

Figure 14: Effect of mt on velocity field U for cooling of plate when Gc = 5,Gr = 5, Sr = 0.2, Sc = 0.22, Pr = 0.71, M = 10, A = 0.1 = B, λ = 0.3, γ = 0.01, s = 0.1, ε = 0.02

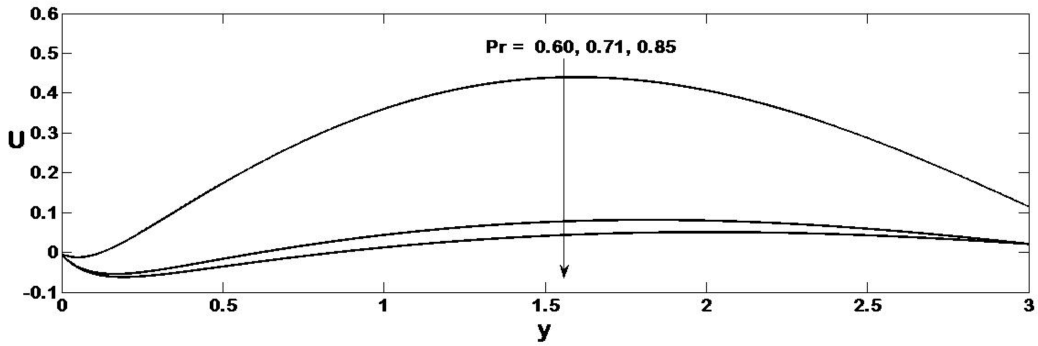

Figure 15: Effect of Pr on velocity field U for cooling of plate when Gc = 5, Gr = 5, Sr = 0.2, Sc = 0.22, $mt = pi/2$, M = 10, A = 0.1 = B, λ = 0.3, γ = 0.01, s = 0.1, ε = 0.02

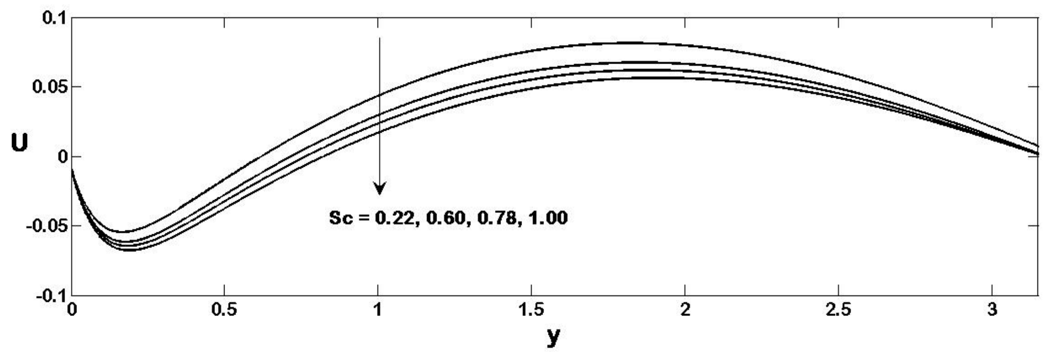

Figure 16: Effect of *Sc* on velocity field U for cooling of plate when Gr = 5, Gc = 5, *Sr* = 0.2, Pr = 0.71, ε = 0.02, M = 10, A = 0.1 = B, Sr= 0.2, γ = 0.01, s = 0.1, $mt = pi/2$

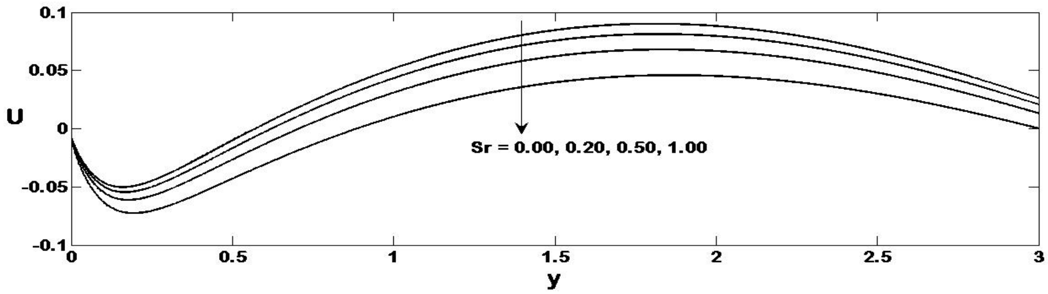

Figure 17: Effect of *Sr* on velocity field U for cooling of plate when Gr = 5,Gc = 5, Sc = 0.22,Pr = 0.71, ε = 0.02, M = 10, A = 0.1 = B, λ = 0.3, γ = 0.01, s = 0.1, $mt = pi/2$

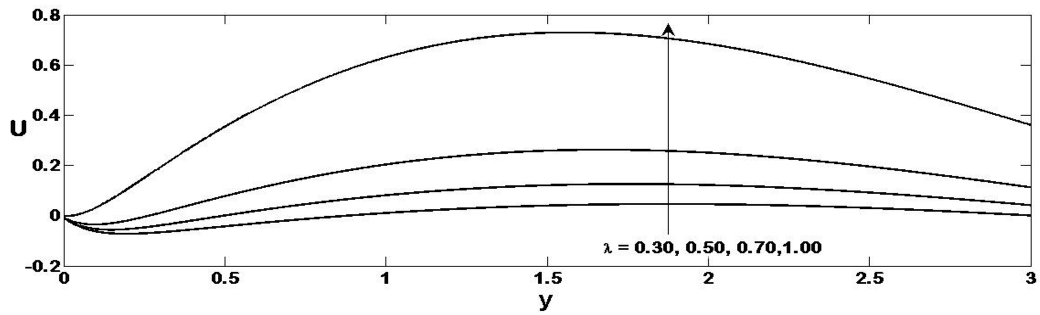

Figure 18: Effect of λ on velocity field U for cooling of plate when Gr = 5, Gc = 5, Sc = 0.22, Pr = 0.71, ε = 0.02, M = 10, A = 0.1 = B, Sr= 0.2, γ = 0.01, s = 0.1, $mt = pi/2$

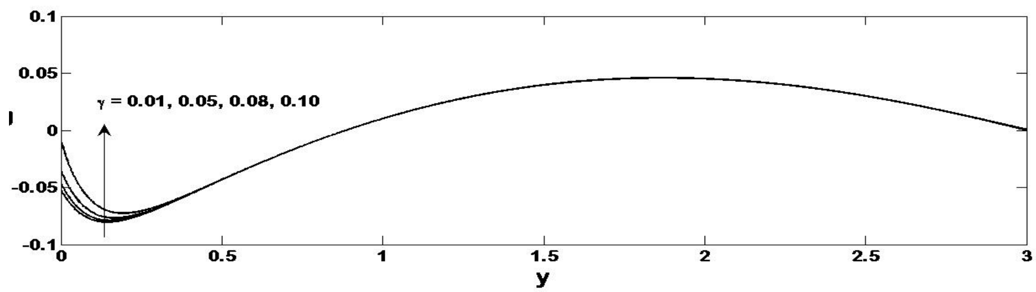

Figure 19: Effect of γ on velocity field U for cooling of plate when Gr = 5, Gc = 5, Sc = 0.22, Pr = 0.71, ε = 0.02, M = 10, A = 0.1 = B, λ = 0.3, Sr = 0.2, s = 0.1, $mt = pi/2$

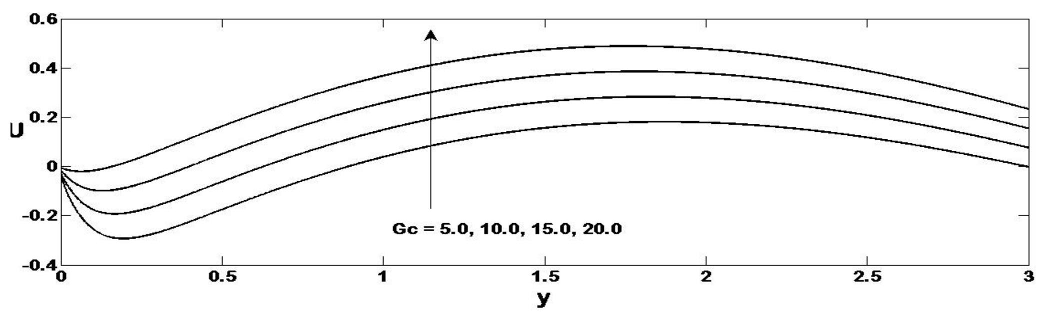

Figure 20: Effect of *Gc* on velocity field U for cooling of plate when Gr = 5, Sr = 0.2, Sc = 0.22, Pr = 0.71, ε = 0.02, M = 10, A = 0.1 = B, λ = 0.3, γ = 0.01, s = 0.1, $mt = pi/2$

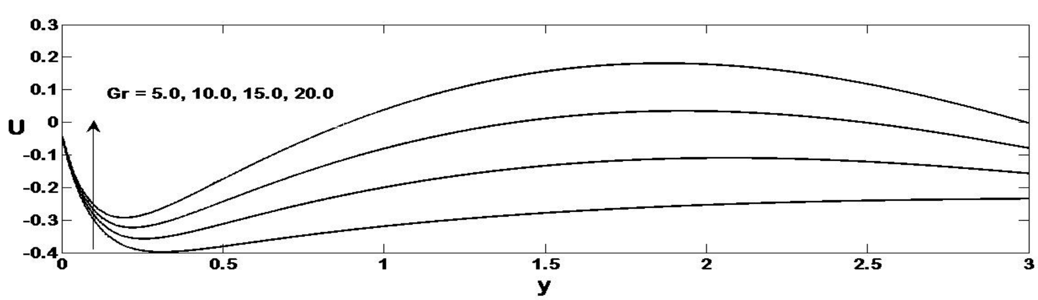

Figure 21: Effect of *Gr* on velocity field U for cooling of plate when Gc = 5, Sr = 0.2, Sc = 0.22, Pr = 0.71, ε = 0.02, M = 10, A = 0.1 = B, λ = 0.3, = 0.01, s = 0.1, $mt = pi/2$

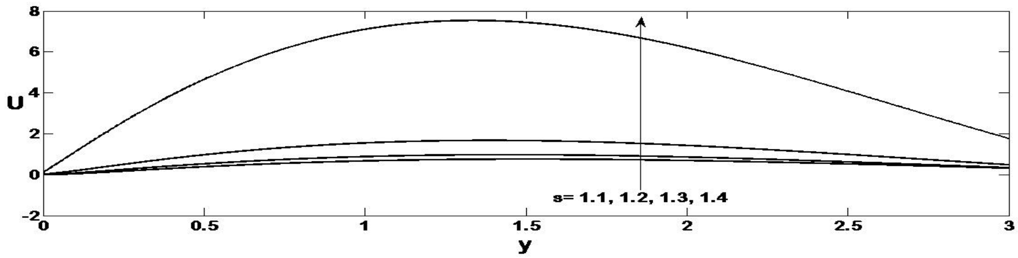

Figure 22: Effect of s on velocity field U for cooling of plate when Gc = 5, Gr = 5, Sr = 0.2, Sc =0.22, Pr = 0.71, ε = 0.02, M = 10, A = 0.1 = B, λ = 0.3, γ = 0.01, $mt = pi/2$

Table 1: Values of skin friction

Pr	λ	s	Sc	Sr	Gr	Gc	M	γ	mt	τ
0.71	0.30	1.10	0.22	0.20	5.00	5.00	5.00	0.01	$pi/2$	1.0392
0.85	0.30	1.10	0.22	0.20	5.00	5.00	5.00	0.01	$pi/2$	4.7869
0.71	0.50	1.10	0.22	0.20	5.00	5.00	5.00	0.01	$pi/2$	0.4457
0.71	0.30	1.20	0.22	0.20	5.00	5.00	5.00	0.01	$pi/2$	0.1433
0.71	0.30	1.10	0.60	0.20	5.00	5.00	5.00	0.01	$pi/2$	1.1969
0.71	0.30	1.10	0.22	0.50	5.00	5.00	5.00	0.01	$pi/2$	1.2051
0.71	0.30	1.10	0.22	0.20	10.00	5.00	5.00	0.01	$pi/2$	2.9421
0.71	0.30	1.10	0.22	0.20	5.00	10.00	5.00	0.01	$pi/2$	0.9785
0.71	0.30	1.10	0.22	0.20	5.00	5.00	6.00	0.01	$pi/2$	0.8689
0.71	0.30	1.10	0.22	0.20	5.00	5.00	5.00	0.02	$pi/6$	0.8964

Table 2: Values of Nusselt number

Pr	λ	s	Sc	Sr	γ	mt	Nu
0.71	0.30	1.10	0.22	0.20	0.01	$pi/2$	4.5119
0.85	0.30	1.10	0.22	0.20	0.01	$pi/2$	-16.4459
0.71	0.50	1.10	0.22	0.20	0.01	$pi/2$	7.9367
0.71	0.30	1.20	0.22	0.20	0.01	$pi/2$	11.0760
0.71	0.30	1.10	0.60	0.20	0.01	$pi/2$	4.5119
0.71	0.30	1.10	0.22	0.20	0.02	$pi/6$	4.3227

Table 3: Values for Sherwood number

Pr	λ	s	Sr	M	γ	mt	Sh
0.71	0.30	1.10	0.20	5.00	0.01	$pi/2$	0.8274
0.85	0.30	1.10	0.20	5.00	0.01	$pi/2$	1.8461
0.71	0.50	1.10	0.20	5.00	0.01	$pi/2$	0.6477
0.71	0.30	1.20	0.20	5.00	0.01	$pi/2$	0.5116
0.71	0.30	1.10	0.20	5.00	0.01	$pi/2$	0.4441
0.71	0.30	1.10	0.50	5.00	0.01	$pi/2$	0.5668
0.71	0.30	1.10	0.20	5.00	0.02	$pi/6$	0.8352

CONCLUSION

We studied the governing equations for boundary layer fluid flow in a channel with heat source parameter and Soret effect. The governing equations were transformed into dimensionless form and perturbation technique was used to solve the problem. Analytical results were obtained using MATlab and presented graphically to illustrate the details of the heat source and Soret and the characteristics relationship with material parameters. From the investigation it was concluded that:

i. The increase of variable parameters $\varepsilon, s, \, and \, \lambda,$ resulted to the increase in temperature and decrease with increasing Pr.
ii. Concentration increases with increase in material parameters $\lambda, mt, Sr, \text{and}\, \varepsilon$ and decreased with Sc .
iii. The velocity increased with increase in material parameters $M, \varepsilon, \lambda, \gamma, Gc, Gr, \text{ and } s$ and decrease with $Sc, Pr \,\text{and}\, Sr.$
iv. The skin friction coefficient increases with increase in material parameters $\lambda, Pr, Sc, Sr, Gc, \text{ and}\, mt$ and decreased with increase in material parameters $s, Gr, M, \text{and}\ \gamma$.
v. Increasing effects of $Pr,$ decreased the Nusselt number, while increasing $\lambda, s \, and \, mt$ increased the Nusselt number with appreciative results.
vi. Sherwood number increased with the increase of material parameter Pr and inversely decreased with increase in $\lambda, s, \, Sc, Sr \, and \, mt$.

NOTATIONS

$A \; and \; B \; are$ constant
C' species concentration in the fluid mol.dm^3
C dimensionless concentration
C_p specific heat at pressure J.kg^{-1}. K^{-1}
D mass diffusion coefficient m^2.s^{-1}
G_c mass Grashof number
G_r thermal Grashof number
g accelerated due to gravity m.s^{-2}
K thermal conductivity J.m^{-1}. K^{-}
T temperature of the fluid near the plate
t' time s
t dimensionless time
u velocity of the fluid in the x-direction m.s^{-1}
u_o velocity of the plate m.s^{-1}
s Heat source
Sc Schmidt number
Pr Prandtl number
M Hartmann number
λ Suction parameter
U dimensionless velocity
x spatial coordinate along the plate
y dimensionless coordinate axis normal to the plate
β volumetric coefficient of thermal expansion K^{-1}
β^* volumetric coefficient of expansion with concentration K^{-1}
ρ density of the fluid kg.m^{-3}
τ dimensionless skin-friction
θ dimensionless temperature
$C_p^{'}$ specific heat at constant pressure
g acceleration due to gravity
$T_\infty^{'}$ temperature of the fluid away from the plate
$T_\omega^{'}$ plate temperature
u', v' velocity component
x', y' coordinate axes normal to the plate
e exponential
$\frac{\partial p}{\partial x}$ pressure term
m frequency oscillation
ε constant
h finite vertical plate.

REFERENCES

Anjalidevi, S.P. and Kandasami (2002). Effects of Chemical Reaction, Heat or and mass Transfer for on Non-Linear MHD Laminar Boundary Layer Flow over a wedge with suction and injection. *International Communication in Heat and Mass Transfer,* **29:**707-716.

Alam, M.S., Rahman, M.M. and Samad, M.A. (2006). Duf0ur and Soret Effects on Unsteady MHD Free Convection and Mass Transfer Flow Past a Vertical Porous Plate, n a Porous Medium. *Nonlinear Analysis; Modeling and Control,* **11(2):** 217–226.

Alam, M.S. and Rahman, M.M. (2005). Dufour and Soret effects on MHD free convective heat and mass transfer flow past a vertical flat plate embedded in a porous medium. *Journal Naval Architecture and Marine Engineering,* **2**(**1):** 55–65.

Brady, J.F. and Acrious, A. (1981). Steady Flow in a Channel or tube with Accelerated surface velocity, an exact solution to the Nervier stokes Equation with reverse flow. *Journal of fluid mechanics,* **112:** 127–150.

Ching-Yang, C. (2010). Soret and Dufour effects on free convection boundary layer over a vertical cylinder in a saturated porous medium. *International Communications in Heat and mass Transfer,* **27(7):** 796-800.

Cheng, W.T. and Lin, H.T. (2002). Non Similarity Solution and correlation of Transient heat transfer in laminar boundary layer flow over a wedge. *International Journal of Engineering Sciences,* **40:** 531–539.

Er-Raki M., Mohammed H., Abdelkhalk A., Mamou, M. and Bounrich, M. (2010). Soret effects on Double -Diffusion Boundary layer flows in a Vertical porous *Cavity. Journal of Porous Media,* **10**: 783-795.

Makinde, O.D., and Olanrewaju, P.O. (2011). Unsteady mixed Convection with Soret and Dufour effects past a Porous plate moving through a Binary mixture of chemically reacting fluid, *Chemical engineering communication,* **198(7):** 920-938.

Muhaimin, R., Hashim, A. and Khemis, B. (2009). On the effect of Chemical reaction, heat and mass transfer on nonlinear MHD Boundary Layer past a porous shrinking sheet with suction theories. *Applied Mechanics,* **36(2):** 101-117.

Makinde, O.D. and Aziz, A. (2011). Boundary layer flow of a nanofluid past a stretching sheet with a convective boundary condition. *International Journal of Thermal sciences,* **50:** 1326-1332.

Postelnicu, A. (2004). Influence of a magnetic field on heat and mass transfer by natural convection from vertical surfaces in porous media considering Soret and Dufour effects. *International Journal of Heat and Mass Transfer* **47**: 1467-1472.

Rafael, C. (2008). Effects of viscous dissipation and radiation on the thermal boundary layer over a nonlinearly stretching sheet. *Physics Letters A.* **372(5):** 631-636.

Shanker B., Prabhakar B. R., and Anand J. R. (2010), Radiation and mass transfer effects on MHD free convective fluid flow embedded in a porous medium with heat generation/absorption. *Indian Journal of Pure and Applied Physics,* **48:** 157-65.

Stanford, S., Sandile, S.M. and Precious S. (2010). The effect of thermal Radiation, Hall currents, Soret, and Dufour on MHD flow by Mixed Convection over a Vertical Surface in Porous Media, *Hindawi Publication Corporation: Mathematical Problems in Engineering,* **ID627475:** 20 pages, doi: 10.1155/2010/627475.

Sakiadis, B.C. (1961). Boundary Layer Behavior on Continuous Solid Surface: I, Boundary–Layer Equation for the dimensional and axis symmetric flow. *AICHE Journal,* **7(1):** 26–28.

Vagravelu, K. and Hadjinicolaou (1999) Convective heat transfer in an electrically conducting fluid at a stretching surface with uniform free Stream. *International Journal of Engineering Science,* **35:** 1237–1244.